Research Square

Preprints are preliminary reports that have not undergone peer review.
They should not be considered conclusive, used to inform clinical practice,
or referenced by the media as validated information.

Repurposing Irosustat for Malaria: Host-Targeted Antiplasmodial Activity via Cholesterol Sulfate Modulation Against Drug-Resistant Plasmodium falciparum

Nguyen Van Truong
Kangwon National University
Tae-Gyu Ahn
Kangwon National University
Tuyet-Kha Nguyen
Kangwon National University
Nguyen Sy Thau
Kangwon National University
Thi Thanh-Hang Chu
Kangwon National University
Sung-Hun Na
Kangwon National University
Won-Sun Park
Kangwon National University
Wan-Joo Chun
Kangwon National University
Feng Lu
Yangzhou University
Jin-Hee Han
Kangwon National University
Seok Jun Moon
Yonsei University
Jeong Taeg Seo
Yonsei University
Eun-Taek Han
ethan@kangwon.ac.kr

Kangwon National University

Research Article

Keywords: Irosustat, cholesterol sulfate, Plasmodium, antimalarial activity

Posted Date: March 24th, 2026

DOI: https://doi.org/10.21203/rs.3.rs-9088819/v1

License: This work is licensed under a Creative Commons Attribution 4.0 International License.
Read Full License

Additional Declarations: No competing interests reported.

Version of Record: A version of this preprint was published at Parasites & Vectors on September 7th, 2026. See the published version at https://doi.org/10.1186/s13071-026-07643-3.

Abstract

Background

The urgent global need for novel antimalarial drugs targeting *Plasmodium falciparum* has intensified due to rising mortality and drug resistance. This study examines a host-directed strategy targeting lipid metabolism by evaluating the antiplasmodial activity of cholesterol sulfate (CS) and Irosustat, a steroid sulfatase inhibitor designed to elevate circulating CS concentrations.

Methods

The antimalarial efficacy of CS was evaluated *in vitro* against chloroquine-sensitive (3D7 and CamWT), chloroquine-resistant (K1 and Dd2), and artemisinin-resistant (CamWTC580Y(+) and Dd2R539T(+)) strains of *P. falciparum*. *In vivo* antimalarial activity of Irosustat was further confirmed using a modified single-dose 4-day test via oral route (PO) in a mouse model against *P. yoelii* (CQ-resistant strain), both as monotherapy and in combination therapy with chloroquine (CQ).

Results

CS effectively inhibited the growth of *P. falciparum* strains, including both drug-sensitive and drug-resistant strains. *In vitro* assays revealed moderate nanomolar IC_{50} values for sensitive strains and low micromolar IC_{50} values for resistant strains. The compound exhibited slow speed clearance and a synergistic effect with artemisinin *in vitro*. *In vivo*, Irosustat achieved more than 80% suppression as monotherapy (40 mg/kg, PO) and more than 90% efficacy in combination with CQ (40/10 mg/kg, PO) against *P. yoelii*, significantly improved survival rates, mean survival days (MSD), body weight, and clinical outcomes. Irosustat exhibits promising antimalarial activity with a favorable oral pharmacokinetic profile.

Conclusions

Future optimization of Irosustat may enhance its antiplasmodial activity, positioning it as a promising candidate for antimalarial drug development.

Background

Malaria, an infectious disease caused by *Plasmodium* parasites, continues to pose a major global health threat, with an estimated 263 million cases and 597,000 deaths reported in 2023 [1]. The increasing prevalence of antimalarial drug resistance, particularly in regions such as Africa, the Americas, and Southeast Asia, has further worsened the situation [1]. Artemisinin-based combination therapies (ACTs)

remain the first-line treatment for uncomplicated *P. falciparum* malaria; however, therapeutic efficacy studies increasingly report treatment failures, even with newer combinations [2, 3, 4, 5]. Thus, there is a critical need to identify novel antimalarial drugs with distinct mechanisms of action and high bioavailability.

Plasmodium parasites heavily depend on host-derived cholesterol and lipid metabolism for growth and replication. This is because parasites lack the full complement of biosynthetic pathways required for de novo cholesterol synthesis. During intraerythrocytic development, *Plasmodium* utilizes cholesterol and other lipids from the host erythrocyte membrane and plasma lipoproteins to undergo membrane biogenesis, nutrient acquisition, and replication. Parasites exploit low-density lipoprotein (LDL) and high-density lipoprotein (HDL) to acquire necessary sterols. In contrast, the parasite remodels host cell membranes and internalizes host-derived phospholipids and fatty acids through endocytic and non-vesicular mechanisms. The requirement for cholesterol and lipids by parasites is even more important during the sexual and liver stages. There is evidence that disruption of host lipid metabolism or inhibition of cholesterol pathways has influenced growth and viability, indicating the vital role of host lipids in parasite development [6, 7, 8].

Consequently, suppression of cholesterol and lipid metabolism in *Plasmodium* presents promise in antimalarial drug development. To be specific, triclosan and thiolactomycin, fatty acid biosynthesis (FAS-II) inhibitors, have exhibited selective antiplasmodial activity *in vitro* and *in vivo* models [9, 10]. Statins, HMG-CoA reductase antagonists, have shown a modest antiplasmodial effect and lack synergy with conventional antimalarial drugs [11]. In addition, host-directed inhibitors of sterol or phospholipid metabolism can indirectly impair *Plasmodium* growth [12, 13]. While targeting cholesterol and lipid metabolism represents a novel avenue for antimalarial drug development, it also faces hurdles, including low potency at safe doses, a lack of synergy with frontline drugs, a high risk of host toxicity, a poor pharmacokinetic profile, and limited *in vivo* efficacy [11, 14].

Irosustat, an orally active and promising steroid sulfatase inhibitor with an oncology safety profile, may provide a novel antimalarial agent. Irosustat has demonstrated its efficacy and promising bioavailability via oral treatment in hormone-dependent cancers such as breast and endometrial cancers. Steroid sulfatase metabolizes not only estrone sulfate and dehydroepiandrosterone sulfate but also cholesterol sulfate and pregnenolone sulfate. Therefore, it would be appropriate to include the conversions of cholesterol sulfate to cholesterol and pregnenolone sulfate to pregnenolone as well. By inhibiting this pathway, Irosustat emerged as the first sulfatase inhibitor and demonstrated potential for breast cancer treatment in both preclinical and clinical studies [15, 16]. In endometrial cancer, patients who received Irosustat (40 mg/day) via oral delivery remained at 36.1% progression-free at six months, with adverse events, primarily of Grade 1 or 2 severity (55.6%) [17].

Despite its favorable safety profile, novel mechanism of action as a steroid sulfatase inhibitor, and potent oral bioavailability, Irosustat has not been evaluated in the context of malaria. Intriguingly, we hypothesized that CS, a naturally occurring sterol sulfate, may possess anti-malarial efficacy, as it is

known to inhibit intracellular cholesterol synthesis by suppressing the mevalonate pathway and concurrently restricting host cell uptake of LDL. To test this host-directed approach *in vivo* by increasing endogenous cholesterol sulfate levels, we used Irosustat, a steroid sulfatase inhibitor [18]. Herein, the antiplasmodial potential of disrupting these pathways was assessed by evaluating CS's *in vitro* activity against drug-sensitive and drug-resistant *P. falciparum* strains, and Irosustat's *in vivo* efficacy in a CQ-resistant *P. yoelii* mouse model. This study provides initial evidence supporting the potential of Irosustat as a novel antiplasmodial agent with a favourable bioavailability profile.

Methods

Ethics statement

All experiments were conducted in accordance with relevant guidelines and regulations, and all protocols involving human samples were approved by the Institutional Ethical Committee of Kangwon National University Hospital (IRB No. KNUH-B-2021-06-034). The animal study was reviewed and approved by the Institutional Animal Care and Use Committee of Kangwon National University and was conducted in accordance with the Ethical Guidelines for Animal Experiments of Kangwon National University (KIACUC-22-133/KNU/KMRL/HET, dated July 1, 2022).

Compounds

Stock solutions (10 mM) of various compounds, including Irosustat (Medchem), CS (Sigma-Aldrich), atovaquone (ATQ) (Sigma—Aldrich) and artemisinin (ART) (Merck) were prepared in 100% DMSO (Sigma—Aldrich), while chloroquine diphosphate salt (CQ) (Sigma—Aldrich) was dissolved in distilled water (DDW).

1. **P. falciparum growth inhibition, combination assay, and kill rate assays in vitro**

P. falciparum parasites, including CQ-sensitive strains (3D7), CQ-resistant strains (K1 and Dd2), an ART-sensitive strain (CamWT), an ART-resistant strain (CamWTC580Y(+)) and a CQ- and ART-resistant strain (Dd2R539T(+))(BEI Resources) [19], were cultured *in vitro* in O+ human red blood cells (RBCs) in RPMI 1640 media (Sigma—Aldrich) supplemented with 100 μM hypoxanthine, 12.5 μg/ml gentamicin, 0.5% (wt/vol) Albumax™ I (Thermo Fisher) and 2 g/L sodium bicarbonate (WELGENE Inc.) at 37°C in in N2 containing 1% O2 and 5% CO2, as described previously[20].

The *in vitro* growth inhibition assay was performed according to a previously reported procedure with modifications [21, 22]. *P. falciparum*, after double synchronization at the early ring stage (R) via 5% sorbitol (wt/vol) treatment [23], was cultured in 96-well plates in a total volume of 100 μl in each well and adjusted to 2% haematocrit and 1% parasitaemia. Different concentrations of compounds dissolved in DMSO (0.1%) were serially diluted and added to the intervention wells. Control wells without treatment were used to assess parasite growth, and wells containing uninfected RBCs were used to exclude

background. Cultures were incubated at 37°C in a humidified culture chamber for at least 72 h (1.5 cycles).

After incubation, the cultures were washed twice with PBS, fixed with 0.05% glutaraldehyde (Sigma-Aldrich) for 10 min, washed twice, stained with SYBR Green I (0.2× dilution, Thermo Fisher) for 10 min, and washed twice with PBS. The samples were analysed with an Accuri C6 flow cytometer (Accuri Cytometers, Inc.). A total of 200,000 cells were analysed, and parasitaemia was determined by gating. The percent inhibition was calculated using the following formula: % growth inhibition = 100-(100 × [intervention well parasitaemia - uninfected well parasitaemia]/[infected well parasitaemia - uninfected well parasitaemia]). The half-maximal inhibitory concentration value (IC_{50}) was determined via the equation (log[inhibitor] vs. response—variable slope [four parameters]) [24]. In each case, at least three independent assays were conducted, each in duplicate, and the data are shown as the mean ± standard deviation.

The fixed ratio isobologram method was used to study *in vitro* interactions between compounds, as described in previous studies [22, 25, 26]. The combinations of ATQ vs. ART and EPO vs. ART were used as reference controls for antagonistic and synergistic interactions, respectively [27, 28]. Drug mixture sets (ATQ vs. ART, EPO vs. ART, CS vs. ART, and CS vs. CQ) with fixed ratios of 1:0, 4:1, 3:2, 2:3, 1:4, 0:1, and 1:1 were serially diluted 10-fold to generate solutions with 7 concentrations. The CS vs. ART and CS vs. CQ sets were dispensed in duplicates in 96-well microplates and incubated with Pf3D7 parasites for 72 h. Growth was measured via FACS, and the percent growth inhibition was calculated as described above. ∑ FIC was computed as the FIC of drug A + the FIC of drug B at each ratio. The mean ∑ FIC was defined as the average ∑ FIC for all studied ratios. An $FIC_{50} < 0.8$ was considered synergistic, whereas an $FIC_{50} > 1.5$ indicates antagonism. In each case, at least three independent assays were conducted, each in duplicate, and the data are shown as the mean ± standard deviation.

In the kill rate assay, the relative bioluminescence intensities were determined as described in previous studies [25]. Briefly, *P. falciparum* NF54-luc-GFP (MRA1217) (BEI Resources) was used to assess parasite viability after 6 h of incubation with serial dilutions of a compound, as measured by bioluminescence. In each case, three independent assays were conducted, each in duplicate, and the data are shown as the mean ± standard deviation.

In vitro effects of inhibitors on parasite morphology

The procedure used to evaluate the effects of the inhibitors on the morphology and stage-specific development of Pf3D7 was based on a previous study [29]. Briefly, to assess the effects of inhibitor treatment on parasite morphology, ring-stage parasites were cultured with DMSO (0.1%) or inhibitors (239.2 nM ATQ, 2.1 μM CS, and 63 nM ART; these concentrations are approximately 3 times the IC_{50}) for 48 h, and the morphology of the parasites was evaluated at various time points (0 h, 12 h, 24 h, 36 h, and 48 h) [29].

Experimental animals

Female BALB/c mice purchased from Orient (Orient Bio), with an average weight of 25 ± 2 g and aged 6–8 weeks, were used in the *in vivo* experiments and maintained in polypropylene cages, with 5 animals in each cage in an animal facility at 25 ± 2°C with a light: dark photoperiod of 12:12 h and 70% relative humidity. The animals were provided a standard laboratory diet and water *ad libitum*. The mice were acclimatized to their experimental environment for 4 days before the experiment started.

Antiplasmodial activity assay in a mouse model

The *in vivo* efficacy was assessed in CQ-resistant *P. yoelii* XL-infected BALB/c mice, using previously described methods with modifications [30]. Female BALB/c mice (5 mice in each group) were inoculated with 10^6 *P. yoelii* XL-infected RBCs taken from passage mice (excluding those in the negative control group). Irosustat was dissolved in the vehicle (10% DMSO, 3% ethanol, 7% Tween-80, and 80% DDW) (VZV), vortexed thoroughly before injection, and administered once daily at 6, 30, 54, and 76 h post-infection. Single-agent treatment consisted of 40 mg/kg Irosustat (PO), while combination therapy included 40 mg/kg Irosustat and 10 mg/kg of CQ in a volume of 200 µl. The remaining groups each received vehicle (200 µl), 10 mg/kg (PO) CQ dissolved in DDW at 6, 30, 54, and 76 h after infection, or no treatment (positive controls), or were not infected (negative controls). Parasitaemia was assessed from 1000 erythrocytes after blood was obtained via the tail vein, stained with Giemsa, and examined under a 100× objective. Twenty-four hours after the last treatment (4 days), the percent suppression was determined using the following formula: % 4-day suppression = 100–100 × parasitaemia (intervention)/parasitaemia (positive). Other parameters, such as adverse events, mean survival days (MSDs), average SRs, clinical parameters, and weights, were also evaluated.

Statistical analysis

The data were analysed using GraphPad Prism (GraphPad Software) and Microsoft Excel 2018 (Microsoft). To compare experimentally measured values across groups, Student's *t*-tests and Mann–Whitney *U*-tests were used. Spearman's correlation was used to examine nonparametric data. $P < 0.05$ was considered to indicate a significant difference.

Results

In vitro inhibitory effects of CS on P. falciparum

CS suppressed the growth of the CQ-sensitive, ART-sensitive Pf3D7 strain in the moderate nanomolar concentrations (696.60 ± 10.04 nM). In addition, CS demonstrated activity against CQ-resistant strains (K1 and Dd2) with IC_{50} values in the micromolar range (21.88 ± 0.02 µM and 22.73 ± 0.01 µM, respectively). The relative IC_{50} values are more than 20-fold that of the CQ IC_{50} ($p < 0.001$) (Table 1).

Table 1
Summary of *in vitro* antimalarial activity of each compound (IC_{50}) against *P. falciparum*.

Strain	Compound	IC_{50}. nM Ring stage[a]	Relative IC_{50}[b]	Resistance index[c]	*P* value[d]
3D7 (CQ, ART-sensitive)	CQ	20.2 ± 1.3	1.0	1	0.000
	ART	19.2 ± 1.1	1.0	1	0.000
	CS	696.6 ± 10.0	34.5	1	-
K1 (CQ-resistant)	CQ	101.4 ± 0.1	1.0	5.0	0.000
	ART	1.7 ± 0.1	0.0	0.2	0.000
	CS	21865.0 ± 21.2	215.6	31.4	-
Dd2 (CQ-resistant)	CQ	76.7 ± 2.2	1.0	3.8	0.000
	ART	6.1 ± 0.5	0.1	0.3	0.000
	CS	22725.0 ± 7.1	296.3	32.6	-
Dd2R539T(+) (CQ, ART-resistant)	CQ	68.6 ± 0.2	1.0	3.4	0.256
	ART	9.2 ± 0.4	0.1	0.3	0.246
	CS	1926.9 ± 1673.2	28.1	2.8	-
Cam WT (ART-sensitive)	CQ	28.3 ± 1.6	1.0	1.4	0.001
	ART	5.8 ± 0.8	0.2	0.3	0.002
	CS	4520.5 ± 253.9	159.7	6.5	-
CamWTC580Y (+) (ART-resistant)	CQ	47.0 ± 1.4	1.0	2.3	0.053
	ART	7.6 ± 0.2	0.2	0.4	0.052

[a]Data are mean ± SD with three independent assays, each performed in duplicates, were collected per experiment. IC_{50} were determined by fitting to the Log vs. response-variable slope equation in GraphPad Prism.

[b]The relative IC_{50} was calculated using CQ as the reference.

[c]Resistance index (RI) is the ratio of IC_{50} for the resistant versus the sensitive strain (3D7).

[d]*P* value was determined by pair comparison CQ vs. CS and ART vs. CS (Student *t*-test).

Strain	Compound	IC_{50}. nM Ring stage[a]	Relative IC_{50}[b]	Resistance index[c]	*P* value[d]
	CS	3251.5 ± 1084.0	69.2	4.7	-
[a]Data are mean ± SD with three independent assays, each performed in duplicates, were collected per experiment. IC_{50} were determined by fitting to the Log vs. response-variable slope equation in GraphPad Prism.					
[b]The relative IC_{50} was calculated using CQ as the reference.					
[c]Resistance index (RI) is the ratio of IC_{50} for the resistant versus the sensitive strain (3D7).					
[d]*P* value was determined by pair comparison CQ vs. CS and ART vs. CS (Student *t*-test).					

Similarly, CS exhibited activity against two ART-resistant strains (CamWTC580Y(+) and Dd2R539T(+)), with IC_{50} values in low micromolar concentrations (3.25 ± 1.08 μM and 1.58 ± 0.80 μM) and a resistance index < 5 (Table 1). In contrast, ART showed slightly higher IC_{50} values against these resistant strains compared to the parental strains CamWT and Dd2 ($p > 0.05$), consistent with previous studies [19]. As expected, Dd2R539T(+) retained resistance to both CQ- and ART but remained sensitive to ONX-0914 (Table 1). Notably, CS demonstrated the lower IC_{50} value in ART-resistant strains (CamWTC580Y(+)) compared to the reverse strain (CamWT) ($p > 0.05$).

Effects of CS on the morphology of parasites in the erythrocytic stage

Plasmodium-infected RBCs treated with ART demonstrated pyknotic nuclei and irreversible chromatin condensation in necrotic or apoptotic cells after 12 h of exposure (Fig. 1a), highlighting that a high rate of parasites were arrested at the ring stage. In contrast, ATQ, the slow-acting agent, did not induce parasite damage in the first cycle. CS caused pyknotic parasites in the late stage after 24 h of treatment, indicating a slow rate of clearance (Fig. 1a).

A kill rate assay was conducted to confirm the compound's fast-acting nature using PfNF54-luc-GFP parasites. Bioluminescence, which indicated parasite viability, was validated after 6 h of treatment (Fig. 1b). While ART, known for rapid clearance, significantly suppressed parasite development at the early ring stage after 6 h of exposure, CS demonstrated lower inhibition of *Plasmodium* proliferation, as with ATQ, indicating slow activity. These findings suggest that CS is a slow-acting inhibitor of *P. falciparum* erythrocytic stages.

Synergistic in vitro with an antimalarial agent

WHO recommended artemisinin combination therapy (ACT) as first-line treatment for uncomplicated falciparum malaria [1]. The fixed ratio isobologram assay evaluated the effects of combining CS with ART and CQ (Fig. 2). The FIC of the combination of ART and CS was 0.71 ± 0.12, indicating *in vitro* synergy and suggesting therapeutic potential (Fig. 2c). Similarly, the isobologram analysis confirmed synergy between CQ and CS with an FIC index of 0.39 ± 0.33 (Fig. 2d).

In vivo antiplasmodial activity in P. yoelii XL-infected mice

Given its potent oral bioavailability and synergistic interaction with CQ, the *in vivo* efficacy of Irosustat was evaluated using a 4-day suppressive test via oral treatment, both as monotherapy and in combination with CQ, in a CQ-resistant *P. yoelii* XL mouse model (Fig. 3a). The compound was administered four doses after inoculation and antiplasmodial activity was evaluated until 14th day post infection (DPI) (Fig. 3a). Irosustat at dose of 40 mg/kg (PO) improved significantly SR and MSD, with SR of 60% and MSD > 13 days after two weeks (Fig. 3b-c). Notably, the Irosustat/CQ combination significantly improves the SR of 80% and MSD of 13.80 ± 0.45 days compared to the untreated group (Fig. 3b-c).

Irosustat significantly suppressed the proliferation of *P. yoelii* after 4 days of treatment, reducing parasitemia to 3.50 ± 0.40% at 40 mg/kg (PO) as monotherapy and to 1.90 ± 0.80% when combined with CQ, compared to positive group ($p < 0.001$) (Fig. 4a). Irosustat sustained antiplasmodial activity after two weeks but did not eliminate parasites completely (Fig. 4a). By 14 DPI, Irosustat suppressed parasitaemia by more than 90% in combination therapy, which was significantly greater than that of monotherapy ($p < 0.05$) (Fig. 4b). CQ at dose of 10 mg/kg demonstrated minimal disruption of *P. yoelli* parasites, consistent with the CQ-resistant phenotype of the strain (Fig. 4a-b). Although not complete parasite clearance, survival in mice treated with Irosustat was better than in untreated mice. To be specific, Irosustat improved body weight and clinical symptoms. No weight loss was observed in mice treated with Irosustat by 14 DPI compared to untreated mice ($p < 0.01$) (Fig. 4c-d). Since parasitemia negatively correlates with body weight [31], this supports the compound's efficacy. Mice administered with Irosustat exhibited fewer symptoms (quiet, ruffled fur, and anaemia) (Fig. 4d). Hepatomegaly and splenomegaly, prominent in the control group, were significantly attenuated in both the Irosustat monotherapy and Irosustat/CQ treatment groups ($p < 0.001$) (Fig. 5a-b). Treated mice reduce liver and spleen sizes without tissue discoloration, reflecting reduced parasite -associated tissue pathology in organs (Fig. 5a-d).

Discussion

The increase of drug-resistant *P. falciparum* strains requires novel antimalarial agents that improve both clinical symptoms and prevent transmission. According to the Medicines for Malaria Venture (MMV), the desired characteristics for Target Candidate Profile 1, Target Candidate Profile 2, and Target Candidate Profile 4 include long-term half-life, prevention of recrudescence, potent oral bioavailability, promising combination, and transmission-blocking [32, 33]. Targeting cholesterol and lipid metabolism has

emerged as a potent approach, as it can disrupt the survival of blood- and liver-stage parasites [6, 7, 8]. Herein, CS, a human cholesterol and lipid inhibitor, demonstrated moderate nanomolar-range anti-plasmodial activity, slow clearance, and *in vitro* synergy with a previous anti-malarial agent during the growth and development of erythrocytic-stage parasites. Its favourable oral bioavailability, along with low toxicity, further supports its potential as a novel antimalarial candidate.

Host-derived cholesterol and lipid metabolism constitute vital pathways for *Plasmodium*, and disruption of these processes has been explored as a potential antimalarial strategy [6, 7, 8]. Previous studies have shown that inhibitors of cholesterol and lipid metabolism, such as triclosan, thiolactomycin, and statins, demonstrated *in vitro* activity in the moderate micromolar range against sensitive and resistant *P. falciparum* strains [9, 10, 11]. Specifically, rosuvastatin inhibited the Pf3D7 and PfDd2 strains with IC_{50} values of 25 and 17 μM, respectively, while atorvastatin exhibited an IC_{50} value of 80 μM [11]. Our study revealed the inhibitory effect of CS against the sensitive Pf3D7 in the moderate nanomolar range (IC_{50} < 800 nM), moderate micromolar against CQ- resistant strains (K1, Dd2) (IC_{50} < 23 μM), and low micromolar against ART- resistant strains (IC_{50} < 4 μM), which was lower than that of statin derivatives. Rat RBCs sequestered greater than 70% of the precursor of CS within 30 min administration, supporting its antiplasmodial activity during the blood stage [34]. However, CS's precursor was partially degraded, with only 48% retained inside RBCs after 24 h, thereby necessitating higher doses to achieve effective parasite killing [34]. Structural optimization to enhance stability, along with evaluation of CS pharmacokinetics and its activity against the sexual and liver stages of *P. falciparum* and other *Plasmodium* strains, could provide evidence for its repurposing as an antiplasmodial agent.

The ability of cholesterol and lipid metabolism inhibitors to synergize with conventional antimalarial drugs has been investigated in previous research [6, 11, 35]. ART and CQ have long served as first-line antimalarials; however, increasing resistance of both drugs has been observed [1]. Combination therapy involving cholesterol and lipid metabolism inhibitors with ART and CQ has been considered as a potential therapy to overcome resistance. Nevertheless, statins (rosuvastatin) demonstrated no synergy effect with CQ and ART against Pf3D7 (FIC > 1) [11]. In contrast, atorvastatin (AVA) showed synergistic effects when combined with quinine against *P. falciparum* strains [36]. A recent study found that coupling primaquine or artesunate to a steroid increases their potency against *P. falciparum* [35]. Notably, CS demonstrated potent synergy with CQ and ART against 3D7 (FIC < 0.8), but slow parasite clearance was observed. This synergy could result from the different modes of action and the half-life time of ART and CS. While ART is characterized by rapid clearance and short half-life (T1/2 = 1–3 h), CS exhibited a longer half-life ($T_{1/2}$ = 31.3 ± 6 h at 5 mg and 28.5 ± 12 h at 20 mg) after oral administration in a human trial [37, 38]. These features support CS as a potent candidate in the ACT regimen as MMV recommendation [32, 33]. Further studies on the potent combination of CS with other conventional drugs, as well as hybridization strategies with ART against different *Plasmodium* strains, may enhance therapeutic development.

A limitation of these inhibitors is their modest efficacy in an *in vivo* model. Previous research revealed that a single regimen of atorvastatin showed no improvement in survival rate, but the prophylactic scheme employing AVA combined with mefloquine alone delayed mouse death, parasitaemia, and cerebral malaria symptoms [39]. In this study, due to the poor pharmacokinetics of CS, Irosustat was used to elevate endogenous CS levels and demonstrated significant improvements in survival, parasitaemia, and growth inhibition, both as monotherapy and in combination with CQ, overcoming CQ-resistant *P. yoelii* in the mouse model. However, the expected long-term protection was not observed. Although it has high oral bioavailability, rapid degradation within red blood cells, and moderate inhibition of *Plasmodium* limited total elimination and relapse protection. In the future, the optimization of structure, dosing, and the combination of Irosustat with ART could be investigated in a rodent malaria model to evaluate its *in vivo* potential.

Conclusions

Repurposing Irosustat for malaria treatment offers a promising antiplasmodial agent, owing to CS's antiparasitic activity against drug-sensitive and drug-resistant strains *in vitro*, its synergistic interactions with standard antimalarial drugs, and its effectiveness upon oral administration. However, major hurdles remain, including minimizing potential toxicity, optimizing structure and hybridization, and addressing the risk of resistance development. These obstacles must be resolved before developing Irosustat as an antimalarial therapy.

Abbreviations

ACTs
Artemisinin-based combination therapies
ART
Artemisinin
ATQ
Atovaquone
AVA
Atorvastatin
CQ
Chloroquine diphosphate salt
CS
Cholesterol sulfate
DDW
Distilled water
DPI
Day post infection
FAS-II
Fatty acid biosynthesis

HDL
High-density lipoprotein
LDL
Low-density lipoprotein
MSD
Mean survival days
PO
Per oral route
RBCs
Red blood cells
SR
Survival rate

Declarations

Ethics approval and consent to participate

All procedures were approved by the Kangwon National University Hospital Ethical Committee (IRB No. KNUH-B-2021-06-034) and the Ethical Guidelines for Animal Experiments of Kangwon National University (KIACUC-22-133/KNU/KMRL/HET, dated July 1, 2022) and conducted according to institutional ethical guidelines.

Consent for publication

Not applicable.

Competing interests

There are no competing interests.

Funding

This study was supported by a National Research Foundation of Korea (NRF) grant (RS-2025-00517986 to E.T.H.) funded by the Ministry of Science, ICT and Future Planning (MSIP), Korea. This research was supported by the Regional Innovation System & Education (RISE) program through the Gangwon RISE Center, funded by the Ministry of Education (MOE) and the Gangwon State (G.S.), Republic of Korea (2025-RISE-10-002 to J.H.H.).

Author Contribution

NVT, SJM, JTS, and ETH were involved in conceiving and designing the experiments and writing the manuscript. NVT, TGA, TKN, NST, TTHC, HUH, and JHH conducted the laboratory work and analyzed the data. SJM and JTS provided reagents/materials. ETH confirmed the authenticity of all the data. All authors approved the content and agreed to be accountable for the work.

Acknowledgements

Not applicable.

Data Availability

Data will be made available upon request.

References

1. WHO. World Malaria Report. 2024.
2. WHO. Strategy to respond to antimalarial drug resistance in Africa. 2022.
3. Zhu L, van der Pluijm RW, Kucharski M, Nayak S, Tripathi J, White NJ, et al. Artemisinin resistance in the malaria parasite, *Plasmodium falciparum*, originates from its initial transcriptional response. Commun Biol. 2022;5 1:274.https://doi.org/10.1038/s42003-022-03215-0.
4. Lucy CO, Lisa Malene R, Lene Sandø E, Vito B, Donal B, Oliver JW, et al. Emerging implications of policies on malaria treatment: genetic changes in the Pfmdr-1 gene affecting susceptibility to artemether-lumefantrine and artesunate-amodiaquine in Africa. BMJ Glob Health. 2018;3 5:e000999. https://ghsite-bmj.vercel.app/content/3/5/e000999.
5. van der Pluijm RW, Imwong M, Chau NH, Hoa NT, Thuy-Nhien NT, Thanh NV, et al. Determinants of dihydroartemisinin-piperaquine treatment failure in *Plasmodium falciparum* malaria in Cambodia, Thailand, and Vietnam: a prospective clinical, pharmacological, and genetic study. Lancet Infect Dis. 2019;19 9:952–61. http://doi.org/10.1016/s1473-3099(19)30391-3.
6. Gulati S, Ekland EH, Ruggles KV, Chan RB, Jayabalasingham B, Zhou B, et al. Profiling the Essential Nature of Lipid Metabolism in Asexual Blood and Gametocyte Stages of *Plasmodium falciparum*. Cell Host Microbe. 2015;18 3:371–81. http://doi.org/10.1016/j.chom.2015.08.003.
7. Coppens I, Vielemeyer O. Insights into unique physiological features of neutral lipids in Apicomplexa: from storage to potential mediation in parasite metabolic activities. Int J Parasitol. 2005;35 6:597–615. https://doi.org/10.1016/j.ijpara.2005.01.009.
8. Labaied M, Jayabalasingham B, Bano N, Cha SJ, Sandoval J, Guan G, et al. Plasmodium salvages cholesterol internalized by LDL and synthesized de novo in the liver. Cell Microbiol. 2011;13 4:569–86. https://doi.org/10.1111/j.1462-5822.2010.01555.x.

9. Yu M, Kumar TRS, Nkrumah LJ, Coppi A, Retzlaff S, Li CD, et al. The Fatty Acid Biosynthesis Enzyme FabI Plays a Key Role in the Development of Liver-Stage Malarial Parasites. Cell Host Microbe. 2008;4 6:567–78. https://doi.org/10.1016/j.chom.2008.11.001.
10. Ralph SA, van Dooren GG, Waller RF, Crawford MJ, Fraunholz MJ, Foth BJ, et al. Metabolic maps and functions of the *Plasmodium falciparum* apicoplast. Nat Rev Microbiol. 2004;2 3:203–16. https://doi.org/10.1038/nrmicro843.
11. Wong RP, Davis TM. Statins as potential antimalarial drugs: low relative potency and lack of synergy with conventional antimalarial drugs. Antimicrob Agents Chemother. 2009;53 5:2212–4. https://doi.org/10.1128/aac.01469-08.
12. Petersen W, Stenzel W, Silvie O, Blanz J, Saftig P, Matuschewski K, et al. Sequestration of cholesterol within the host late endocytic pathway restricts liver-stage *Plasmodium* development. Mol Biol Cell. 2017;28 6:726–35. https://doi.org/10.1091/mbc.E16-07-0531.
13. Itoe MA, Sampaio JL, Cabal GG, Real E, Zuzarte-Luis V, March S, et al. Host cell phosphatidylcholine is a key mediator of malaria parasite survival during liver stage infection. Cell Host Microbe. 2014;16 6:778–86. https://doi.org/10.1016/j.chom.2014.11.006.
14. Konaklieva MI, Plotkin BJ. Targeting host-specific metabolic pathways-opportunities and challenges for anti-infective therapy. Front Mol Biosci. 2024;11:1338567. https://doi.org/10.3389/fmolb.2024.1338567.
15. Biernacki K, Ciupak O, Daśko M, Rachon J, Kozak W, Rak J, et al. Development of Sulfamoylated 4-(1-Phenyl-1H-1,2,3-triazol-4-yl) phenol Derivatives as Potent Steroid Sulfatase Inhibitors for Efficient Treatment of Breast Cancer. J Med Chem. 2022;65 6:5044–56. https://doi.org/10.1021/acs.jmedchem.1c02220.
16. Palmieri C, Januszewski A, Stanway S, Coombes RC. Irosustat: a first-generation steroid sulfatase inhibitor in breast cancer. Expert Rev Anticancer Ther. 2011;11 2:179–83. https://doi.org/10.1586/era.10.201.
17. Pautier P, Lobbedez FJ, Melichar B, Kutarska E, Hall G, Reed N. A Phase II Multicenter Randomized Open-Label Study of Oral Steroid Sulphatase (STS) Inhibitor Irosustat (BN83495) Versus Megestrol Acetate (MA) in Women with Advanced/Recurrent Endometrial Cancer (EC). AnnOncol. 2012;23:ix329. https://doi.org/10.1016/S0923-7534(20)33559-6.
18. Nam LB, Kim SJ, Nguyen TK, Jeong CY, Lee JY, Lee JS, et al. Cholesterol sulfate as a negative regulator of cellular cholesterol homeostasis. Mol Cells. 2025;48 6:100209. http://doi.org/10.1016/j.mocell.2025.100209.
19. Straimer J, Gnädig NF, Witkowski B, Amaratunga C, Duru V, Ramadani AP, et al. Drug resistance. K13-propeller mutations confer artemisinin resistance in *Plasmodium falciparum* clinical isolates. Science. 2015;347 6220:428–31. https://doi.org/10.1126/science.1260867.
20. Trager W, Jensen JB. Continuous culture of *Plasmodium falciparum*: its impact on malaria research. Int J Parasitol. 1997;27 9:989–1006. https://doi.org/10.1016/s0020-7519(97)00080-5.

21. Muh F, Lee S-K, Hoque MR, Han J-H, Park J-H, Firdaus ER, et al. In vitro invasion inhibition assay using antibodies against *Plasmodium knowlesi* Duffy binding protein alpha and apical membrane antigen protein 1 in human erythrocyte-adapted P. knowlesi A1-H.1 strain. Malar J. 2018;17 1:272. https://doi.org/10.1186/s12936-018-2420-4.
22. Van Truong N, Nguyen TK, Thau NS, Chu TH, Sanaullah B, Venkataramaiah C, et al. Dual-targeting proteasome inhibitor ONX-0914 demonstrates potent antiplasmodial activity for malaria treatment. Int J Parasitol Drugs Drug Resist. 2025;29:100613. https://doi.org/10.1016/j.ijpddr.2025.100613.
23. Lambros C, Vanderberg JP. Synchronization of *Plasmodium falciparum* erythrocytic stages in culture. J Parasitol. 1979;65 3:418–20. https://doi.org/10.2307/3280287.
24. Sebaugh JL. Guidelines for accurate EC50/IC50 estimation. Pharm Stat. 2011;10 2:128 – 34. https://doi.org/10.1002/pst.426.
25. Lawong A, Gahalawat S, Ray S, Ho N, Han Y, Ward KE, et al. Identification of potent and reversible piperidine carboxamides that are species-selective orally active proteasome inhibitors to treat malaria. Cell Chem Biol. 2024;31 8:1503-17.e19. https://doi.org/10.1016/j.chembiol.2024.07.001.
26. Watson QD, Carias LL, Malachin A, Redinger KR, Bosch J, Bardelli M, et al. Human monoclonal antibodies inhibit invasion of transgenic *Plasmodium knowlesi* expressing *Plasmodium vivax* Duffy binding protein. Malar J. https://doi.org/10.1186/s12936-023-04766-1.
27. Souza GE, Bueno RV, de Souza JO, Zanini CL, Cruz FC, Oliva G, et al. Antiplasmodial profile of selected compounds from Malaria Box: in vitro evaluation, speed of action and drug combination studies. Malar J. https://doi.org/10.1186/s12936-019-3069-3.
28. Dogovski C, Xie SC, Burgio G, Bridgford J, Mok S, McCaw JM, et al. Targeting the cell stress response of *Plasmodium falciparum* to overcome artemisinin resistance. PLoS Biol. 2015;13 4:e1002132. https://doi.org/10.1371/journal.pbio.1002132.
29. Prasad R, Atul, Kolla VK, Legac J, Singhal N, Navale R, et al. Blocking *Plasmodium falciparum* development via dual inhibition of hemoglobin degradation and the ubiquitin proteasome system by MG132. PLoS One. 2013;8 9:e73530. https://doi.org/10.1371/journal.pone.0073530.
30. Fidock DA, Rosenthal PJ, Croft SL, Brun R, Nwaka S. Antimalarial drug discovery: efficacy models for compound screening. Nat Rev Drug Discov. 2004;3 6:509–20. https://doi.org/10.1038/nrd1416.
31. Friedman JF, Kurtis JD, Ramadhan M, Opollo M, Lanar DE, Duffy PE. Malaria Is Related to Decreased Nutritional Status among Male Adolescents and Adults in the Setting of Intense Perennial Transmission. J Infect Dis. 2003;188 3:449–57. https://doi.org/10.1086/376596.
32. MMV. Target product profiles (TPPs) and target candidate profiles (TCPs) for malaria medicines. 2018.
33. Burrows JN, Duparc S, Gutteridge WE, Hooft van Huijsduijnen R, Kaszubska W, Macintyre F, et al. New developments in anti-malarial target candidate and product profiles. Malar J. 2017;16 1:26. https://doi.org/10.1186/s12936-016-1675-x.
34. Ireson CR, Chander SK, Purohit A, Parish DC, Woo LW, Potter BV, et al. Pharmacokinetics of the nonsteroidal steroid sulphatase inhibitor 667 COUMATE and its sequestration into red blood cells in

rats. Br J Cancer. 2004;91 7:1399–404. https://doi.org/10.1038/sj.bjc.6602130.

35. Fraser M, Curtis B, Phillips P, Yates PA, Lam KS, Netzel O, et al. Harnessing cholesterol uptake of malaria parasites for therapeutic applications. EMBO Mol Med. 2024;16 7:1515–32. https://doi.org/10.1038/s44321-024-00087-1.
36. Parquet V, Henry M, Wurtz N, Dormoi J, Briolant S, Gil M, et al. Atorvastatin as a potential anti-malarial drug: in vitro synergy in combinational therapy with quinine against *Plasmodium falciparum*. Malar J. 2010;9 1:139. https://doi.org/10.1186/1475-2875-9-139.
37. White NJ. Qinghaosu (artemisinin): the price of success. Science. 2008;320 5874:330–4. https://doi.org/10.1126/science.1155165.
38. Stanway SJ, Purohit A, Woo LW, Sufi S, Vigushin D, Ward R, et al. Phase I study of STX 64 (667 Coumate) in breast cancer patients: the first study of a steroid sulfatase inhibitor. Clin Cancer Res. 2006;12 5:1585–92. https://doi.org/10.1158/1078-0432.ccr-05-1996.
39. Souraud J-B, Briolant S, Dormoi J, Mosnier J, Savini H, Baret E, et al. Atorvastatin treatment is effective when used in combination with mefloquine in an experimental cerebral malaria murine model. Malar J. 2012;11 1:13. https://doi.org/10.1186/1475-2875-11-13.

Figures

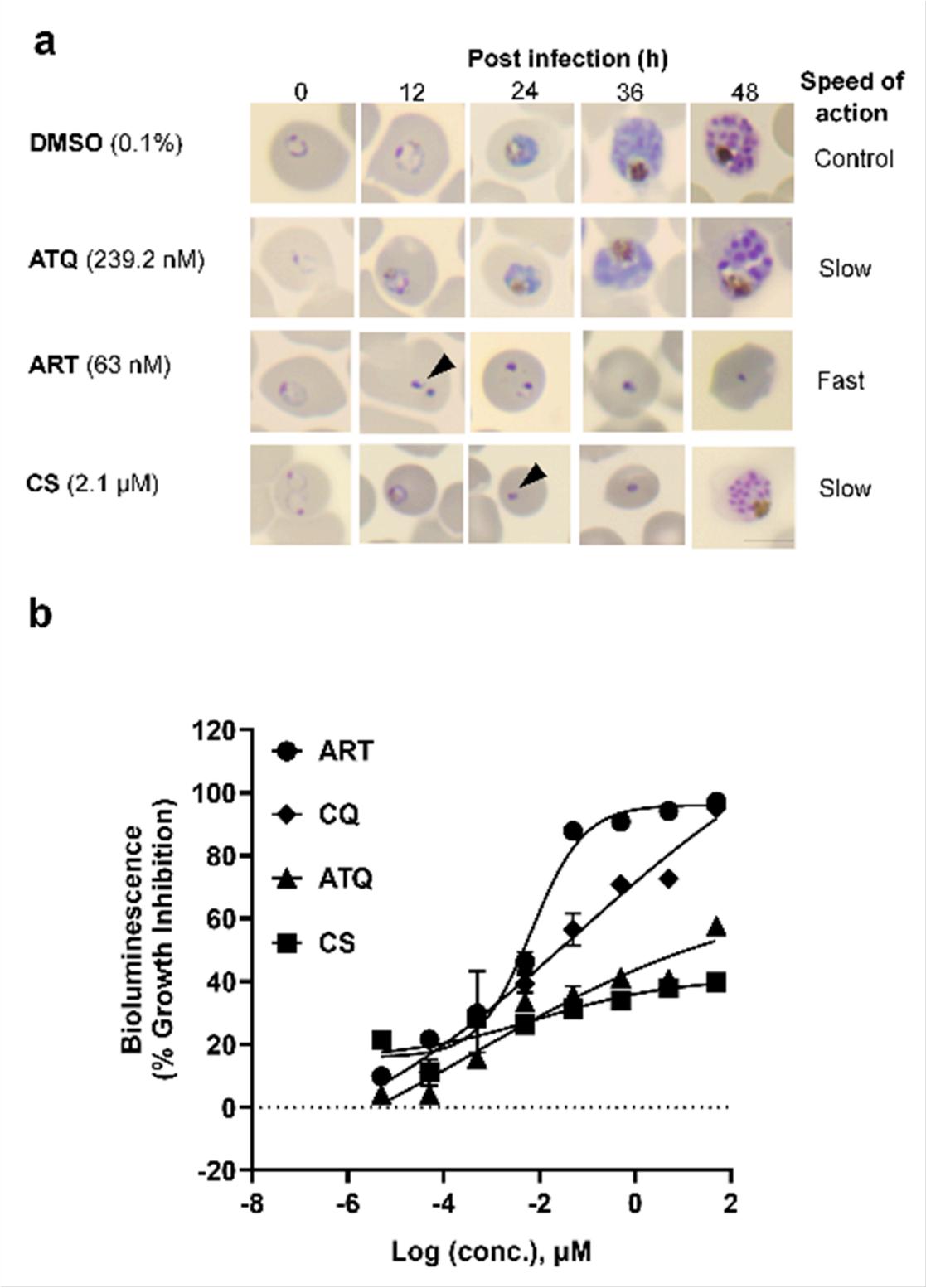


Figure 1

Morphologies of the CS-treated parasites, inhibitor kill rates. **a** Morphology of CS-treated *Pf*3D7 parasites. Parasites were cultured with 0.1% DMSO or the indicated inhibitors (239.2 nM ATQ, 63 nM ART, and 2.1 μM CS concentrations nearly 3 times greater than the corresponding IC_{50}) for 48 h, and their morphologies on Giemsa-stained smears were evaluated at various time points. ART treatment resulted in pyknotic morphology early, at 12 h, whereas CS treatment did so after 24 h. The black arrows indicated

pyknotic vacuoles. Scale bars = 5 μm. **b** Kill rate assay. NF54-luc-GFP parasites were incubated with inhibitors for 6 h. The measured bioluminescence signals were normalized to those of the untreated control and converted to a growth inhibition rate. ART (fast-kill) and ATQ (slow-kill) were used as controls for treatment.

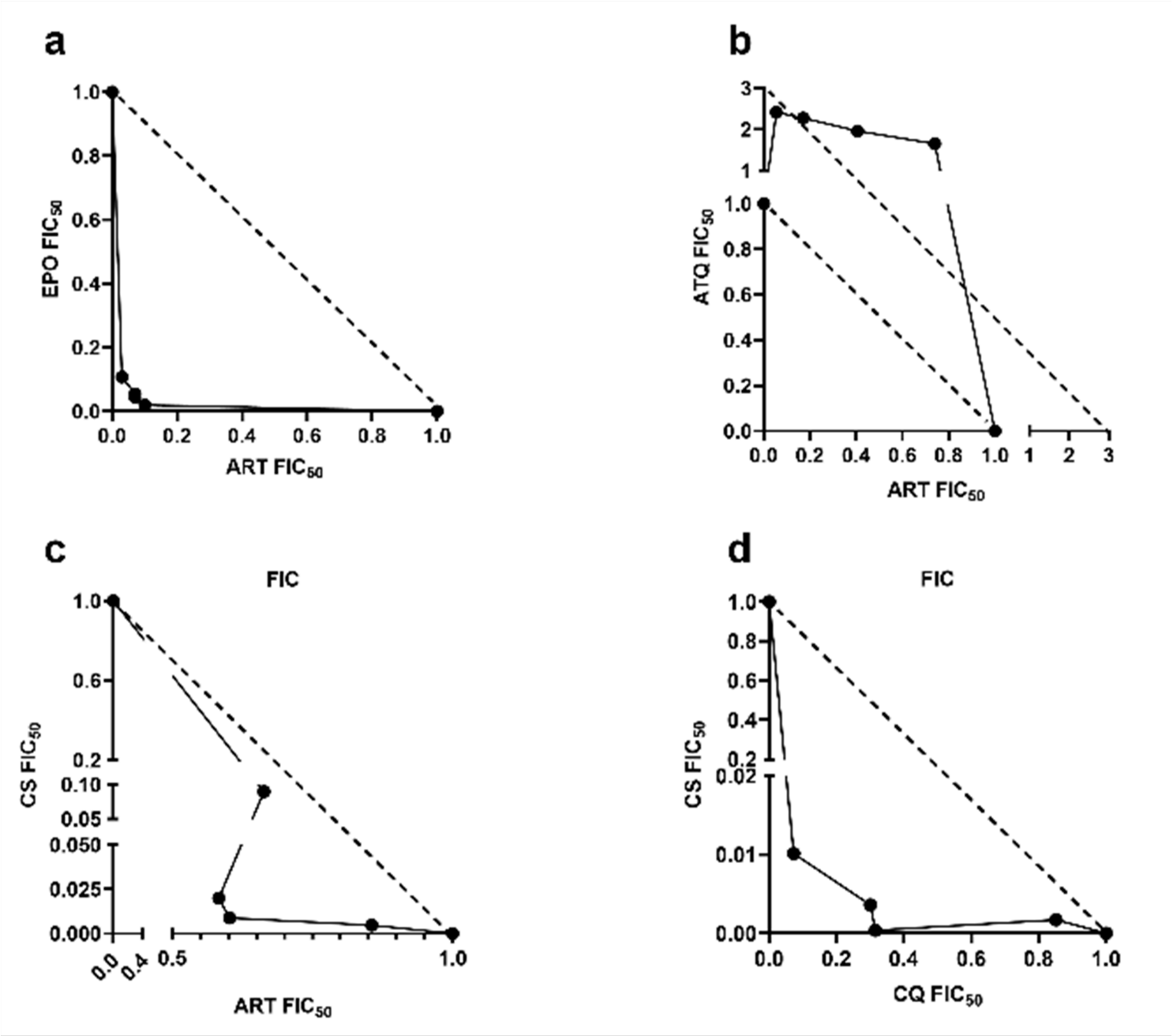


Figure 2

Fixed ratio isobolograms of ART vs EPO, ART vs ATQ, CS vs ART, and CQ against 3D7 (CQ- and ART-sensitive strain). ART vs EPO was used as a control for synergistic interaction, while ART vs ATQ was used as a control for antagonistic interaction. **a** Isobologram showing interaction between ART vs EPO against 3D7. **b** Isobologram showing interaction between ART vs ATQ against 3D7. **c** Isobologram showing interaction between CS vs ART against 3D7. **d** Isobologram shows interaction between CS vs

CQ against 3D7. ATQ vs ART served as the control for antagonistic interaction ($\sum FIC_{50}$ = 1.75 ± 0.39) while EPO vs ART served as the synergistic effect ($\sum FIC_{50}$ = 0.12 ± 0.05). CS demonstrated synergism with ART and CQ ($\sum FIC_{50}$ = 0.71 ± 0.12 and 0.39 ± 0.33), respectively (*n*=3 biological replicates based on technical duplicates). $\sum FIC_{50} < 0.8$ is considered synergistic, whereas $\sum FIC_{50} > 1.5$ indicates antagonism. The IC_{50} was calculated in Prism 10.2.2 via the equation (log[inhibitor] vs. response-variable slope [four parameters]).

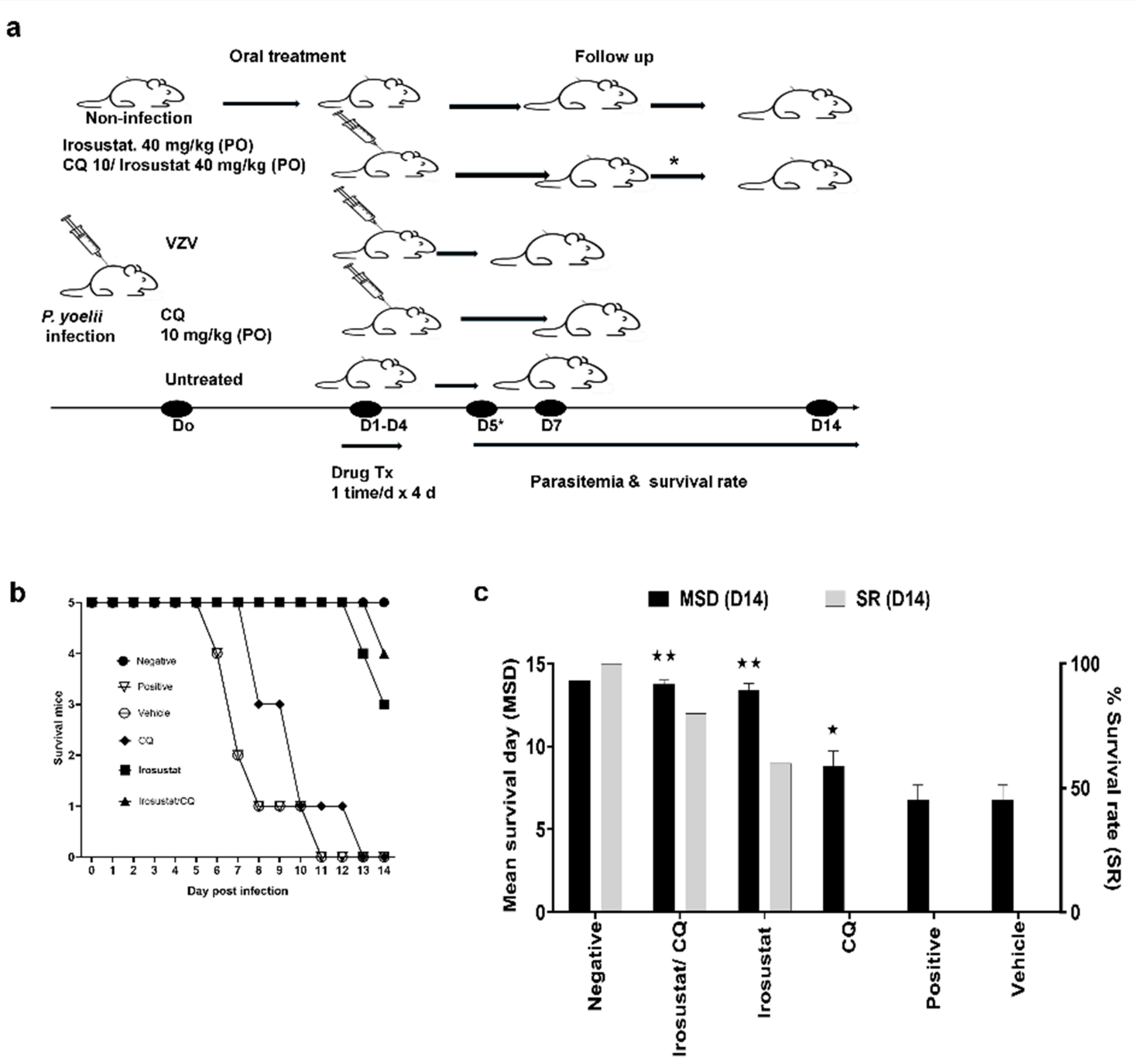


Figure 3

Combination of the mean survival days (MSDs) and survival rate (SR) after treatment with Irosustat via oral route, as determined using curative treatment (4-day suppression). **a** Flowchart of the *in vivo* assay. D-0 (+6 h), D-1, D-2, and D-3, the days of treatment after inoculation. The mice were treated with a single dose of Irosustat (40 mg/kg, PO) or with a combination of CQ (10 mg/kg, PO) for 4 days after inoculation. Mice were monitored for 14 days. **b** Survival of mice in the group treated with CQ (10 mg/kg), Irosustat (40 mg/kg), Irosustat/CQ combination at 14 days of post-infection (DPI), and negative (uninfected mice), positive (infected mice), and vehicle groups. **c** MSDs and SRs for each group at 14 DPI. Irosustat increased the MSD and survival rate of mice after treatment, both as monotherapy and in combination with other agents. Each group included 5 mice.

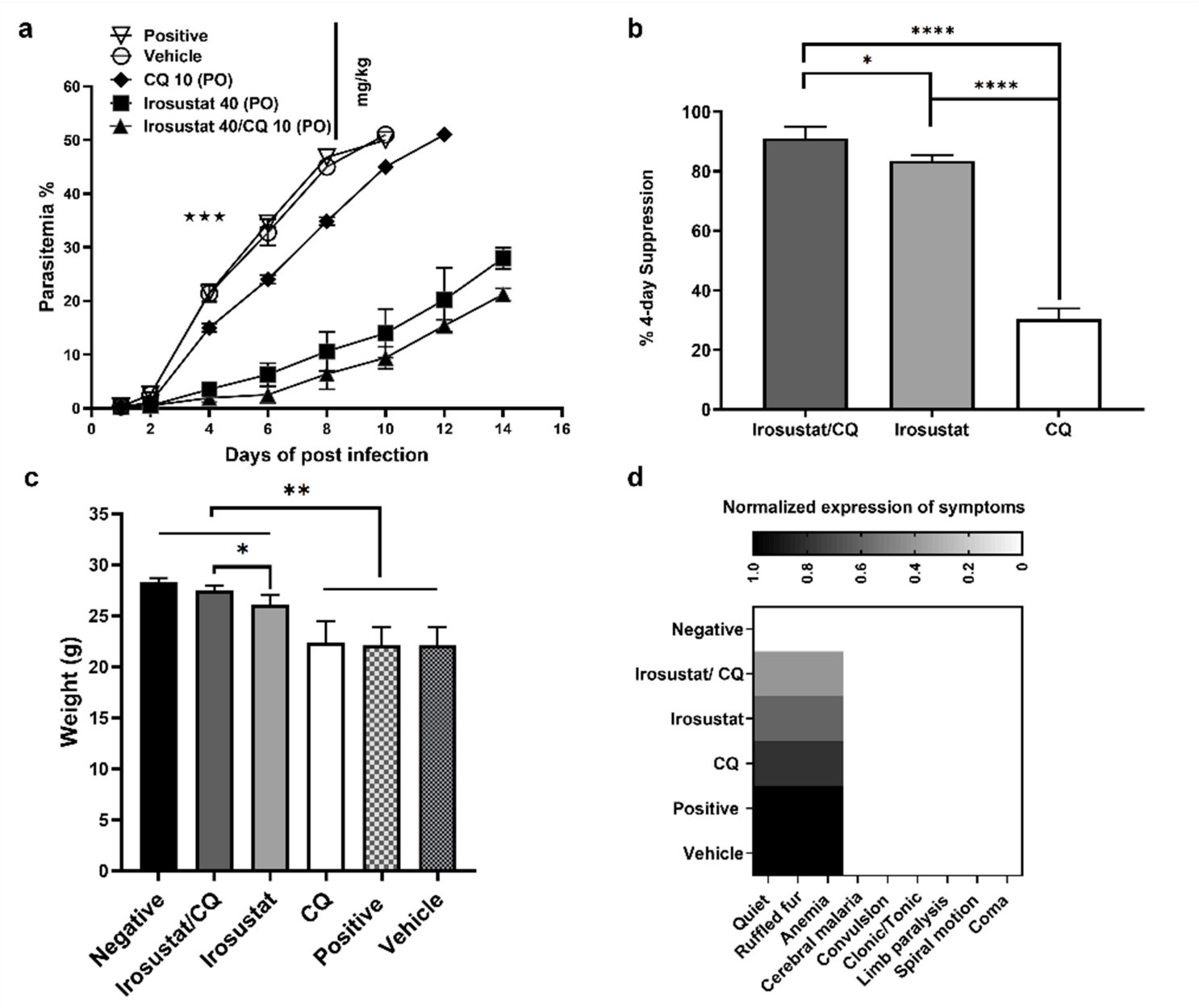


Figure 4

Effect of Irosustat administered via oral routes on parasitaemia suppression, weights, and clinical symptoms. **a** Parasitaemia follow-up at 14 DPI. At least 1000 red blood cells were counted under a microscope to evaluate parasitaemia. **b** Rate of parasitaemia suppression after 4 days of treatment calculated using the following equation: (% suppression=100-100´(parasitaemia of intervention/parasitaemia positive). Intervention (infected mice with treatment), positive (infected mice without treatment). Irosustat significantly suppressed the parasite proliferation in combination with CQ, greater than in monotherapy ($p < 0.05$). **c** Weights of the mice at 14 DPI. Compared with mice receiving no treatment, those receiving oral Irosustat showed improvements in body weight. **d** Clinical symptoms. Symptom expression was normalized by calculating the percentage of mice with symptoms within each group relative to the total number of mice in that group. Statistical significance calculated using a two-tailed *t*-test (* $p< 0.01$, ** $p < 0.001$). The data are shown as the means ± standard deviations. The error bars indicate the standard deviation (SD) of the mean. Each group included 5 mice.

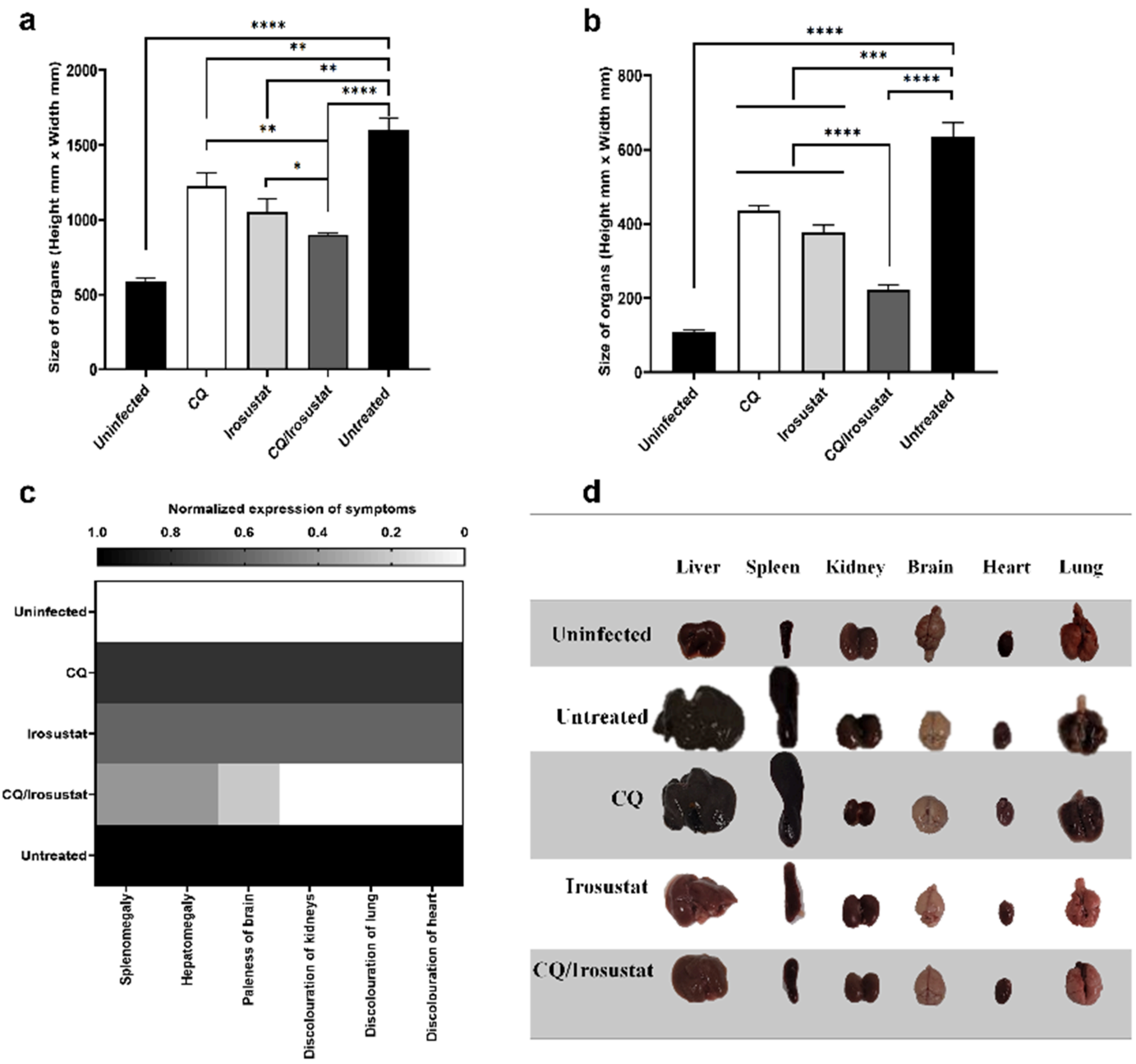


Figure 5

Effects of Irosustat on the organs' pathology in *P. yoelii*-infected mice. **a-b** Liver and spleen sizes. Organ size was calculated as height × width (mm). Mice treated with Irosustat alone or in combination with CQ had smaller livers and spleens than untreated mice. **c**Gross pathological features of organs (brain, heart, lung, liver, kidneys, and spleen) after sacrifice (colour and size). **d** Images of the brain, heart, lung, liver, kidney, and spleen. Scale bar = 5 mm. Negative (uninfected mice), positive (infected mice). Organs were collected from 3 mice per group. **a-b**Statistical significance calculated using a two-tailed *t*-test is expressed relative to the positive and vehicle (infected mice and infected mice treated with vehicle) using asterisks (** $p < 0.001$, *** $p < 0.0001$).

Supplementary Files

This is a list of supplementary files associated with this preprint. Click to download.

- Graphicabstract.tif